A Modeling and Control approach for a cubic AUV

Benoit Clement * **Yang Rui** ** **Ali Mansour** * **Li Ming** **

* *Lab-STICC, UMR CNRS 6285, ENSTA Bretagne, 29806 Brest Cedex 9, France (e-mail: benoit.clement@ensta-bretagne.fr).*
** *Ocean University of China, College of Engineering, Qingdao 266100, China (e-mail: yangrui@ouc.edu.cn)*

Abstract: This paper presents a control synthesis methodology for a cubic AUV. The modeling part is based on CFD calculation and the control part is based on H_∞ theory, nonlinear compensation, Smith compensation and Kalman filter. It is presented and adapted to Ciscrea AUV for heading control. A comparison with PID controller is given with simulations and sea tests.

Keywords: Robust Control, AUV, application, modelling

1. INTRODUCTION

Underwater vehicles have a large variety of types and they are widely involved in undersea surveillance, inspection and survey missions (Clement (2013b)). Typically, AUVs and gliders are common with a torpedo shape for long range missions, and Human Occupied Vehicles (HOVs) as well as Remote Operating Vehicles (ROVs) are generally of a cubic shape used for hovering tasks. Note that, for some specific applications: undersea pipeline inspection, offshore infrastructure surveillance and large vessel maintenance, a small size cubic AUV is preferred. Indeed, small AUVs can be deployed to explore areas which are not accessible to HOVs and ROVs. Meanwhile, the cubic shaped AUVs enjoy more degrees of freedom than torpedo-shaped AUVs. Indeed, they can hover and enter complex underwater spaces.

Achieving good maneuverability of small AUV depends on two key factors: an accurate hydrodynamic model and an advanced control system. Yamamoto (Aug., 2001) pointed out that a model-based control system is more efficient if the dynamics of the vehicle are modeled to some extent. Meanwhile, Ferreira et al. (April, 2012) show that an empirical linear model often fails to represent the dynamics of the AUV over a wide operating region. In this work, we adopt our previously published model (Yang et al. (2015)).

Regardless of modeling issues, the value of a model-based control approach depends on how robust and efficient the control scheme can adopt the hydrodynamic model. Potential trends of current methods focus on faster controllers to assist the pilot or the autopilot with better accuracy. Optimal controllers can reduce propelling actions to save the battery power as well as to increase the propeller lifespan. Moreover, numerous uncertainties should be considered, including parameter variations, nonlinear hydrodynamic damping effects, sensor transmit delays and ocean current disturbances. In robotic competitions (SAUC-E and eu-Rathlon), it has been shown that a PID yaw controller was less efficient for a low mass AUV. Consequently, advanced control algorithms should be involved, such as the adaptive control scheme by Maalouf et al. (Feb., 2013), interval analysis approach by Jaulin and Le Bars (2012). Note that robust control schemes are shown to be successfully by Feng and Allen (Feb., 2004) and Roche et al. (pp. 17-24, Sep., 2010) for torpedo-shaped AUVs. In this work, we appointed the CISCREA AUV shown in Figure 1 and main characteristics are given in Table 1.

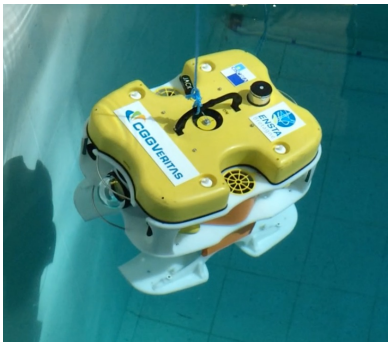

Fig. 1. CISCREA AUV picture in the test pool of ENSTA Bretagne

Table 1. CISCREA AUV main characteristics

Size	0.525m (L) 0.406m (W) 0.395m (H)
Weight in air	15.56 kg (without payload and floats)
Degrees of Freedom	Surge, Sway, Heave and Yaw
Propulsion	2 vertical and 4 horizontal propellers
Speed	2 knots (Surge) & 1 knot (Sway, Heave)
Depth Rating	50m
On-board Battery	2-4 hours

This work is organized as follows. AUV main notions, Ciscrea model and its derivative equations for control design are presented in Section 2. A control scheme based on nonlinear feedback and H_∞ optimization is proposed in Section 3. Section 4 shows the Matlab simulation results of H_∞ and PID controllers. In addition, the improved H_∞ scheme adaption and sea tests are presented. It is important to note that the validation is performed from

simulation to real envirionment like it has been done for other robots (Clement (2013a)).

In this paper, we propose a original embedded control structure simple model oriented; using Kalman filters, the unmeasured and noisy system states are estimated. A Smith compensator is introduced to compensate the magnetic compass delay. The system uncertainties are dealt with H_∞ theory. The experiment and simulation results show the advantages of the proposed CFD model based H-infinity methods compared with PID controller.

2. AUV MODELING

This section is dedicated to describe the AUV modeling notions as well as the dynamic and hydrodynamic parameters of Ciscrea AUV. A yaw model is derived in this section for robust heading control design. Note that, modeling data in this section comes from our previous CFD works (Yang et al. (2015)).

2.1 AUV Modeling Notions

Ciscrea AUV dynamics are represented marine vehicle formulation by Fossen (2002) and by the Society of Naval Architects and Marine Engineers (SNAME (April 1950)). Positions, angles, linear and angular velocities, force and moment definitions are reflected in Tab 2. The position vector η, velocity vector ν and force vector τ are defined as follows:

$$\eta = [x, y, z, \phi, \theta, \psi]^T;$$
$$\nu = [u, v, w, p, q, r]^T;$$
$$\tau = [X, Y, Z, K, M, N]^T$$

Table 2. The notation of SNAME

	Positions and Angles	Velocities	Forces and Moments
Coordinate	NED-frame	B-frame	B-frame
Surge	x	u	X
Sway	y	v	Y
Heave	z	w	Z
Roll	ϕ	p	K
Pitch	θ	q	M
Yaw	ψ	r	N

According to Fossen (2002), rigid-body hydrodynamic forces and moments can be linearly superimposed. Therefore, the overall non-linear underwater model can be characterized by two parts, the rigid-body dynamic (1) and hydrodynamic formulations (2) (hydrostatics included):

$$M_{RB}\dot{\nu} + C_{RB}(\nu)\nu = \tau_{env} + \tau_{hydro} + \tau_{pro} \quad (1)$$
$$\tau_{hydro} = -M_A\dot{\nu} - C_A(\nu)\nu - D(|\nu|)\nu - g(\eta) \quad (2)$$

Table 3 describes the parameters of this model. Due to the size of the matrices and the figures needed to show all the numerical values, the reader can refear to the paper dedicaded to modeling (Yang et al. (2015)).

For the Ciscrea AUV, the rigid-body mass inertia matrix M_{RB} is simplified due to symmetry. Here, $r_G = [x_G, y_G, z_G]^T$ is the vector from O_b (origin of B-frame) to CG (center of gravity).

C_{RB} and C_A contribute to the centrifugal force. Note that a practical way to calculate these two matrices using

Table 3. Nomenclature of the notations

Parameter	Description
M_{RB}	AUV rigid-body mass and inertia matrix
M_A	Added mass matrix
C_{RB}	Rigid-body induced coriolis-centripetal matrix
C_A	Added mass induced coriolis-centripetal matrix
$D(\|v\|)$	Damping matrix
$g(\eta)$	Restoring forces and moments vector
τ_{env}	Environmental disturbances (wind, waves and currents)
τ_{hydro}	Vector of hydrodynamic forces and moments
τ_{pro}	Propeller forces and moments vector

M_{RB}, M_A and ν is introduced in Marine System Simulator (MSS (2010)). In our case, these two matrices can be neglected due to the low speed to be considered, $C(v) \approx 0$. For an AUV with neutral buoyancy, the weight W is approximately equal to the buoyancy force B.

For Ciscrea AUV, CB (the buoyancy center) and CG are located using trials and errors method by adding and removing the payload and floats. The marine disturbances, such as the wind, waves and currents are related to the environmental effect τ_{env}. However for a deep sea underwater vehicle, only current should be considered since wind and waves have negligible effects. Two hydrodynamic parameters added mass, $M_A \in \mathbb{R}^{6\times6}$, and damping, $D(|\nu|) \in \mathbb{R}^{6\times6}$, should be carefully involved in the AUV model. Added mass is a virtual conception representing the hydrodynamic forces and moments. Any accelerating emerged-object would encounter this M_A due to the inertia of the fluid. For a cubic-shaped AUV, added mass in some directions are generally larger than the rigid-body mass as explained by Yang et al. (May, 2014). Damping in the fluid consists of four parts: Potential damping $D_P(|\nu|)$, skin friction $D_S(|\nu|)$, wave drift damping $D_W(|\nu|)$ and vortex shedding damping $D_M(|\nu|)$. For the CISCREA AUV, quadratic damping is the main dynamic nonlinearity of the system (Yang et al. (May, 2014)).

2.2 Ciscrea model

For applying the methodology to the Ciscrea AUV, Mass inertia matrix, M_{RB}, is calculated using PRO/ENGINEER software, and added mass matrix, M_A, is calculated using WAMIT^{TM} based on radiation/diffraction program. Finally, STAR-CCM+^{TM} software and real world experiments are conducted to estimate the relationship among damping forces, damping moments, vehicle velocities and angular velocities. In Yang et al. (May, 2014, 2015), second order polynomial lines are implemented to approximate the relationship between damping and velocities.

2.3 Yaw model

Without loss of generality, we only present the robust controller in yaw direction. The rotational model is simplified as in (3) (neglecting buoyancy and gravity). Definitions and parametric values, such as inertia and damping coefficients, are listed in Table 4. Note that, all the parameters have uncertainties, as they are either measured or numerically calculated. The uncertainties will be carefully discussed and treated using H_∞ solution in section 3.

$$(I_{YRB} + I_{YA})\ddot{x}_r + D_{YN}|\dot{x}_t|\dot{x}_r + D_{YL}\dot{x}_r = \tau_i \quad (3)$$

Table 4. Rotational model parameters for yaw direction

Parameter	Description	Value
I_{YRB}	Rigid-body inertia	$0.3578kg \cdot m^2$
I_{YA}	Added mass inertia	$0.138kg \cdot m^2$
D_{YN}	Nominal quadratic damping factors	Ideal 0.2496
D_{YL}	Nominal linear damping factors	Ideal 0.021
$\dot{x}_r$	Angular Velocity	0 to 4rad/s
τ_i	Torque input	0 to $6N \cdot m$
τ_{com}	Compensation Torque	0 to $6N \cdot m$
$\dot{x}_{r0}$	Equilibrium velocity	0 to 4rad/s
D_{YND}	CFD quadratic damping factors	0.1479
D_{YLD}	CFD linear damping factors	0.0013
D_{YLA}	Artificial linear factors	<Motor limit (select 1.2)

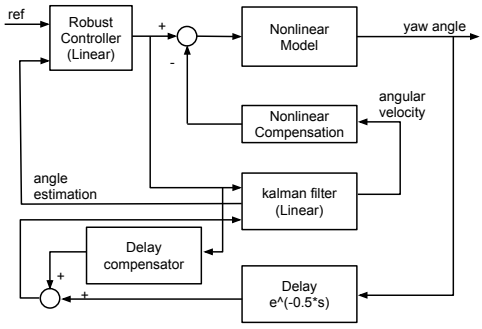

Fig. 2. Ciscrea H_∞ heading control scheme with nonlinear and delay compensations, Kalman filter and linear H_∞ controller.

3. CONTROL STRUCTURE

In this section, an original struture is proposed. It is based on H_∞ theory, nonlinear compensation, Smith compensation and Kalman filter. It is presented and adapted to Ciscrea AUV for heading control. The proposed structure is given on figure 2. One can see the various parts of the control.

We propose a framework to :

- change the nonlinear yaw model into a linear system with uncertainties based on previous modeling works (here is an important contribution that shows the links between control and modeling);
- tune a Kalman filter if only few sensors are used (compass in our case);
- tune a Smith compensator for the delay due to the low cost sensor;
- solve a H_∞ controller for the linear system.

3.1 Nonlinear compensation

In this part, we discuss the nonlinear problem without concern of parametric uncertainties, such as inertia and damping coefficient errors. As shown in Yang et al. (May, 2014), damping is a major nonlinear component in the AUV model. Therefore, in Figure 3, we propose to compensate nonlinear behaviors using the CFD yaw model, as feedback for real world propellers.

The nonlinear compensation is given in equation (4).

$$\tau_{com} = (D_{YLA} - D_{YLD} - D_{YND}|\dot{x}_r|)\dot{x}_r \tag{4}$$

where:

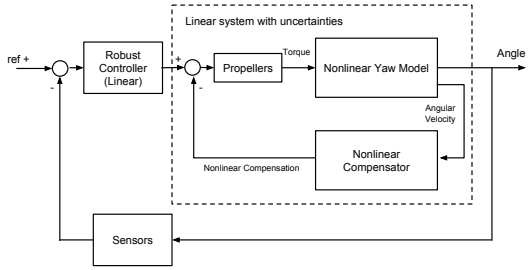

Fig. 3. Nonlinear Compensator allows linear synthesis

- D_{YLA} is the artificial linear factor given in Tab 4.
- D_{YND} and D_{YLD} are CFD damping estimations.

The linear model result of compensation is given in equation (5).

$$(D_{YLA} + (D_{YN}|\dot{x}_r| - D_{YND}|\dot{x}_r| + D_{YL} - D_{YLD}))\dot{x}_r + (I_{YRB} + I_{YA})\ddot{x}_r = \tau_i \tag{5}$$

The term $\delta = D_{YN}|\dot{x}_r| - D_{YND}|\dot{x}_r| + D_{YL} - D_{YLD}$ is calculated as an uncertainty added to D_{YLA}. Generally, this δ is small comparing to D_{YLA}. If we calculate δ using that:

$$\dot{x}_r \in [-4, 4] \text{ rad/s; } D_{YLA}\text{=1.8; } D_{YN}\text{=0.2496;}$$
$$D_{YL}\text{=0.021; } D_{YND}\text{=0.1479; } D_{YLD}\text{=0.0013;}$$

we can consider that D_{YLA} is a nominal parameter which has a dynamic uncertainty of 23.7%.

$$(I_{YRB} + I_{YA})\ddot{x}_r + (D_{YLA} + \delta)\dot{x}_r = \tau_i \qquad \delta \in [-0.4265, 0.4265] \tag{6}$$

At the end, the proposed model, equation (6), is a linear system with uncertainties. Therefore, H_∞ approach is feasible for this model as it is proposed in figure 3.

3.2 Linear controller: H_∞ synthesis

Let us consider the following classical state space representation of a linear time invariant (LTI) system:

$$\begin{bmatrix} \dot{x} \\ z \\ y \end{bmatrix} = \begin{bmatrix} A & B_1 & B_2 \\ C_1 & D_{11} & D_{12} \\ C_2 & D_{21} & D_{22} \end{bmatrix} \begin{bmatrix} x \\ w \\ u \end{bmatrix} \tag{7}$$

where $x \in \mathbb{R}^n$ is the state vector, $u \in \mathbb{R}^{m_2}$ the control input, $y \in \mathbb{R}^{p_1}$ system output, $w \in \mathbb{R}^{m_1}$ the external input vector, $z \in \mathbb{R}^{p_2}$ the error vector. The robust design process is to find a LTI feedback controller K, such that the closed-loop system remains stable and is able to achieve given performances in presence of uncertainties (Gu et al. (2005); Zhou and Doyle (1998)). Generally, cost functions for finding K are represented by H_∞ norms of the closed-loop transfer functions from w to z, as seen in equation (8).

$$\min_{K stable} \left\| \begin{matrix} W_p(I+GK)^{-1} \\ W_e(I+GK)^{-1} \\ W_u K(I+GK)^{-1} \end{matrix} \right\|_\infty < \gamma \tag{8}$$

Here, K is the robust controller in Figure 4, and G is the linear nominal yaw model. The nominal model is derived from the linear fractional transformation (LFT) technique,

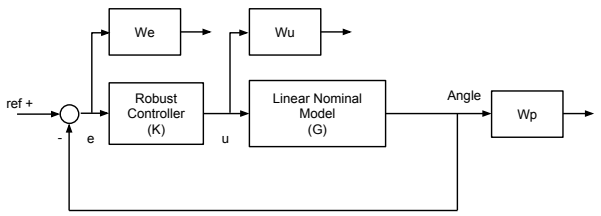

Fig. 4. H_∞ synthesis structure: weighting functions, nominal model, controller.

which separates uncertainties into an individual block (Gu et al. (2005)).

In H_∞ theory, weighting functions are introduced for setting control specifications. Generally, it is difficult to get the accurate frequency characteristics of external input signals. Therefore, weighting functions are sometimes the upper bound that covers original signals. For example, the weighting function W_p, which represents the frequency characteristics of the external disturbance, is used to describe output disturbance rejection ability. Satisfying the above norm inequality indicates that the closed-loop system indeed reduces the disturbance effects to a prescribed level.

Finding appropriate weighting functions is critical and difficult, trials are necessary for a successful robust control design. In this application, we choose a structure with three weighting functions as it can be seen in Figure 4. W_e is chosen as a reference tracking error requirement, W_u represents the input disturbance rejection. W_p, which restricts the output disturbance, is the same specification with W_e, but with different objectives.

Weighting function parameters are selected according to equations (9) to (11). W_u is selected to be a very small scalar ($Gu = 0.01$) for disturbance rejection. We choose W_e and W_p according to Gu et al. (2005) and Roche et al. (pp. 17-24, Sep., 2010), carefully considered the robust margins, tracking error (1%) and fast response.

$$W_p(s) = 0.95\frac{s^2 + 1.8s + 10}{s^2 + 8s + 0.01} \tag{9}$$

$$W_e(s) = 0.5\frac{s + 0.92}{s + 0.0046} \tag{10}$$

$$W_u(s) = 0.01 \tag{11}$$

To solve the H_∞ problem, one can use the Riccati method or Linear Matrix Inequality (LMI) approach Zhou and Doyle (1998). Usually, we prefer to choose the LMI approach, as it requires less initial conditions (Gu et al. (2005)). The resulting transfers are given in Figure 5.

3.3 Delay compensation

First, underwater vehicles might not be equipped with enough sensors to detect all the states, such as the angular velocity $\dot{x}_r$. In addition, the magnetic compass may encounter serious signal delay and noise injection. Therefore, we propose to use a CFD model based kalman filters, numerically estimating unmeasured as well as noisy states. In addition, model based compensation algorithms are

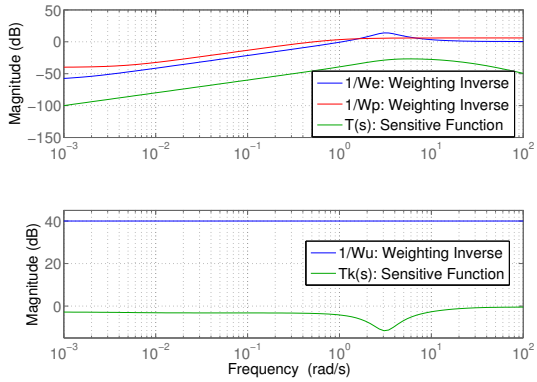

Fig. 5. Sensitivity Functions and inverse of weighting functions

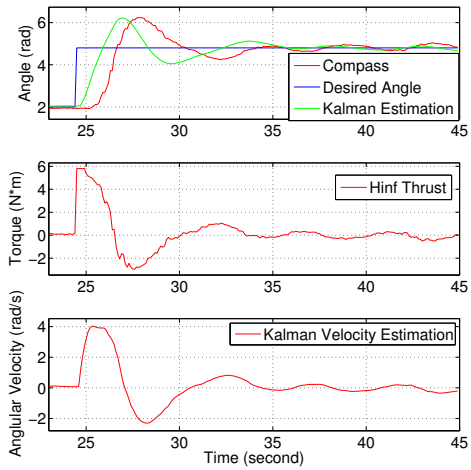

Fig. 6. Ciscrea H_∞ heading control delay and noise problem

recommended to deal with the sensor delay. The proposed H_∞ approach is completed as it is shown in Figure 2.

In order to reveal the magnetic compass delay as well as noise injections on the rotational motion of CISCREA AUV, A less tuned H_∞ heading controller was demonstrated in Figure 6. Among the Kalman angle estimation and magnetic compass output, an obvious $0.5s$ delay was observed. In this case, the delay lead to distinct heading control oscillations. Meanwhile, there exist noise efforts on the control output to propellers.

For Ciscrea heading control application, a classical Smith compensator was introduced by Zhong (2006) to compensate the magnetic compass delay, see Figure 7 and equation (12).

$$P(s) = G_0(s) - G_0(s)e^{-0.5s} \tag{12}$$

The main idea is to estimate current delay free output y from the nominal model $G_0(s)$ and real output $ye^{(-0.5+\delta)s}$. Figure 8 shows the H_∞ heading control simulation results using Smith predictor compensation.

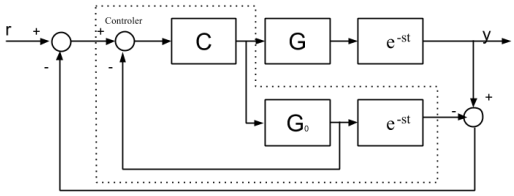

Fig. 7. Smith Predictor struture for delay compensation

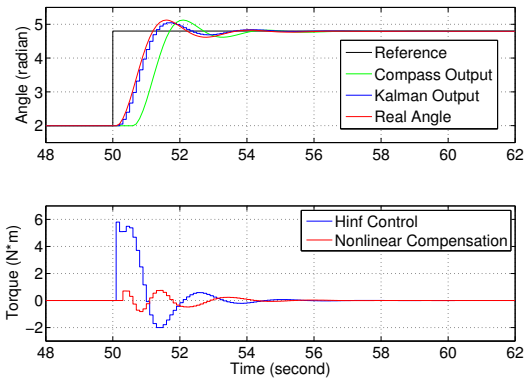

Fig. 8. Improved Ciscrea H_∞ heading controller (Smith Compensation)

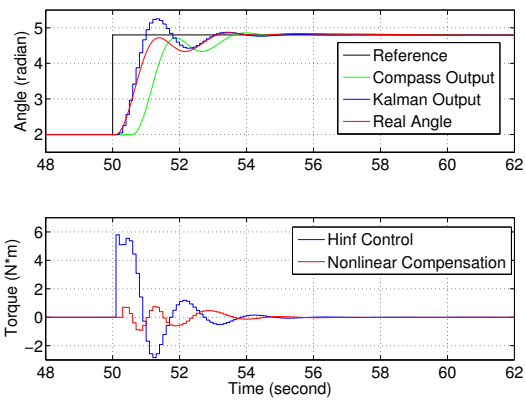

Fig. 9. Improved Ciscrea H_∞ heading controller (Kalman Compensation)

In addition, as robust controller is insensitive to compensation errors, we are enlighten to propose another compensation scheme using Kalman angular velocity estimation ($\dot{x}_r$), see equation (13).

$$y = P(s)u + ye^{(-0.5+\delta)s}, y = K_c\dot{x}_r + ye^{(-0.5+\delta)s}, K_c > 0 \quad (13)$$

A $K_c = 0.57$ was tuned which has an efficient compensation result in Figure 9.

4. SIMULATION AND EXPERIMENTS

4.1 Heading control simulation

In the simulation, $I_{YRB} + I_{YA}$ and D_{YLA} are considered to be two varying parameters, which have respectively 30% and 40% ($>$ 23.7%) of variations. In Figure 10,

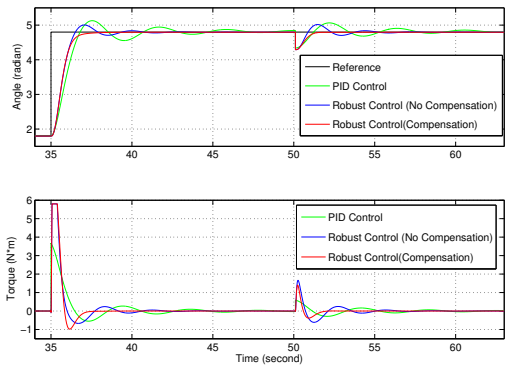

Fig. 10. Step Response and Propellor Output on Nominal Yaw Model

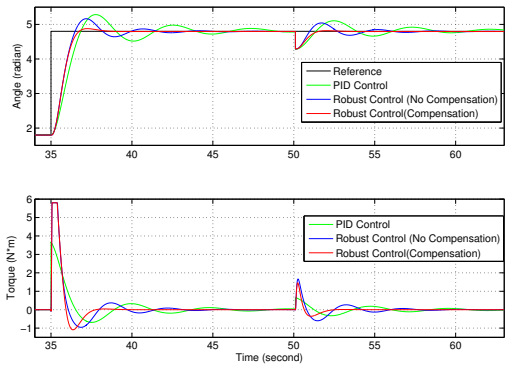

Fig. 11. Step Response and Propellor Output with 30% of interia variation

step responses of three scenarios are represented: PID control, damping compensated H_∞ approach and bare H_∞ control. From the simulation comparison, we can conclude that compensated H_∞ controller handles the nonlinearity with the fastest response. Compensated H_∞ controller has no overshot and oscillations during the rotation process. Tracking error achieves the specification less than 1%. To emphasize the speed and robustness of our approach, we inject a small disturbance of $0.5rad$ on the output at $50s$. Figure 11 shows the robust performance of our controller handling a yaw model with 30% inertia variations.

4.2 Ciscrea Sea Test

The proposed control scheme has been validated on Ciscrea in sea tests, and its results are compared with a traditional PID approach, respectively shown in Figures 12 and 13. First, H_∞ heading controller is faster than PID scheme (even with low battery conditions). Second, there is no nonlinearity induced oscillations in the control output, and the tracking accuracy is better. Third, from the propeller thrust signal, we can determine that the magnetic compass noise and disturbances are well rejected, while PID is less efficient to handle those uncertainties. Finally, the characteristics of our controller result in an optimal and smooth propulsion, which saves the battery energy, and allows to increase the working range.

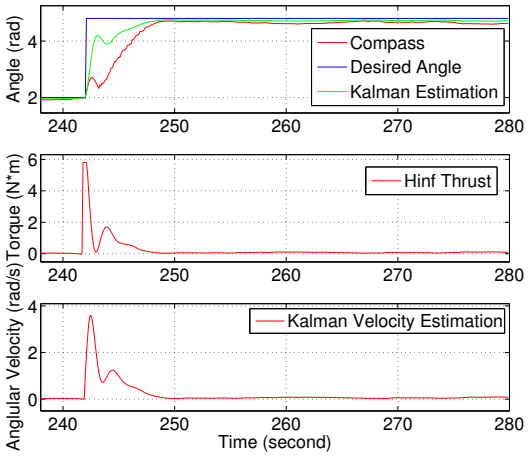

Fig. 12. Ciscrea H_∞ heading control sea experiment (Kalman compensation)

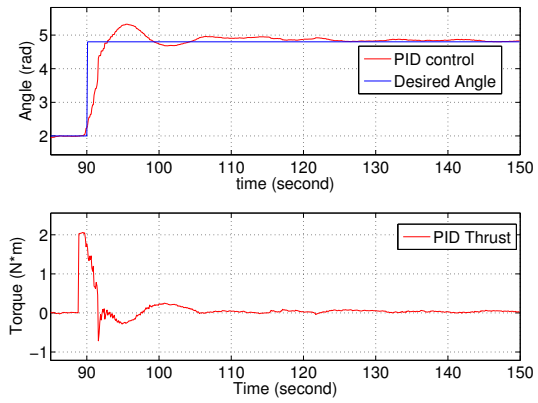

Fig. 13. Ciscrea PID heading control sea experiment (Brest Port)

5. CONCLUSION

We have presented an efficient CFD model based H_∞ control method to improve the motion performance of AUVs with uncertainties. It has been validated on the heading control scenario of low-mass and complex-shaped Ciscrea AUV in sea tests. Experimental and simulation results have proved that CFD model based H_∞ has many advantages comparing to PID controller:

- faster in time response for a step demand;
- free from nonlinearity induced oscillations and overshoot (CFD compensation);
- free from sensor delay induced oscillations (Delay compensation); efficient noise and disturbance rejection (Kalman filter and H_∞ perfomance constraints);
- not sensitive to parametric variation uncertainties (Robustness);
- optimal and smooth propulsion orders.

The proposed robust heading control application demonstrates a high quality AUV motion control solution, and finally it uses only one compass as feedback sensor.

ACKNOWLEDGEMENTS

This work was supported by the China Scholarship Council, Ocean University of China and ENSTA Bretagne.

REFERENCES

Clement, B. (2013a). Control algorithms for a sailboat robot with a sea experiment. In *Proceedings of the 9th IFAC Conference on Control Applications in Marine Systems*. Osaka, Japan.

Clement, B. (2013b). A marine robotics point of view for oceanography. In *Innovation and Blue Growth Symposium*. Qingdao, China.

Feng, Z. and Allen, R. (Feb., 2004). Reduced order h_∞ control of an autonomous underwater vehicle. *Control Engineering Practice*, 12(12), 1511–1520.

Ferreira, B.M., Matos, A.C., and Cruz, N.A. (April, 2012). Modeling and control of trimares auv. In *12th International Conference on Autonomous Robot Systems and Competitions*, 57–62. Portugal.

Fossen, T.I. (2002). *Marine control systems: Guidance, navigation and control of ships, rigs and underwater vehicles*. Marine Cybernetics Trondheim.

Gu, D.W., Petkov, P.H., and Konstantinov, M.M. (2005). *Robust Control Design with MATLAB*. Springer.

Jaulin, L. and Le Bars, F. (2012). An interval approach for stability analysis: Application to sailboat robotics. *IEEE Transaction on Robotics,*, 27(5), 282 – 287.

Maalouf, D., Tamanaja, I., Campos, E., Chemori, A., Creuze, V., Torres, J., Rogelio, L., et al. (Feb., 2013). From pd to nonlinear adaptive depth-control of a tethered autonomous underwater vehicle. In *5th Symposium on System Structure and Control*. Grenoble, France.

MSS (2010). Marine systems simulator (2010) viewed 01.02.2014. [online]. available: http://www.marinecontrol.org.

Roche, E., Sename, O., and Simon, D. (pp. 17-24, Sep., 2010). Lpv/h_∞ varying sampling control for autonomous underwater vehicles. In *4th IFAC Symposium on System, Structure and Control*. Delle Marche, Italy.

SNAME (April 1950). Nomenclature for treating the motion of a submerged body through a fluid. *The Society of Naval Architects and Marine Engineers, Technical and Reserach Bulletin*, 1–15.

Yamamoto, I. (Aug., 2001). Robust and non-linear control of marine system. *International Journal of Robust and Nonlinear Control*, 11(13), 1285–1341.

Yang, R., Clement, B., Mansour, A., Li, H., Li, M., and Wu, N. (May, 2014). Modeling of a complex shaped underwater vehicle. In *Proceedings of the 14th IEEE International Conference on Autonomous Robot Systems and Competitions*. Espinho, Portugal.

Yang, R., Clement, B., Mansour, A., Li, M., and Wu, N. (2015). Modeling of a complex-shaped underwater vehicle for robust control scheme. *Journal of Intelligent and Robotic Systems*, 1–16. doi:10.1007/s10846-015-0186-2.

Zhong, Q. (2006). *Robust control of time delay systems*. Springer, Berlin.

Zhou, K.M. and Doyle, J.C. (1998). *Essentials of robust control*. Prentice hall.